

*CHAPTER III
PETROGRAPHICAL
AND
MINERALOGICAL
CHARACTERISTICS*

CHAPTER (III)

PETROGRAPHICAL AND MINERALOGICAL CHARACTERISTICS

3.1 Introduction

This chapter deals with the petrography and mineralogy of the studied Eocene rocks and their weathering products (Gehannam Formation and Quaternary deposits). The main task is to identify the type of clay and non clay minerals as well as chemical characteristics because of their effect on the engineering properties. The collected samples from Gehannam Formation and Quaternary deposits have been subjected to a series of procedures namely X-ray diffraction (XRD), thin section investigation, scanning electron microscopy (SEM) and X-ray fluorescence (XRF).

3.2 Clay content and foundation problems

From engineering point of view, type of clay minerals plays an important role in many foundation problems when the soil or base materials exposed to water, the soil or base materials swell when wetted and shrink when dried out (Gramko, 1974). Such volume changes in soils were important because they determine settlements due to shrinkage, heave due to swelling and contribute to deformations caused by shear stress (Mitchell and Soga, 2005).

3.3 Relation between mineral constituents and engineering parameters

Clay minerals have different affinities for the absorption of moisture, which cause shrinkage and swelling (Thomas et al., 2000) and (Hudyma and Burcin Avar, 2006). The charge distribution and cation

species determine the swell potential of a soil clay mineral. Clay minerals have a net permanent negative charge (layer charge) resulting from vacancies or solid state substitutions of cations in the tetrahedral and octahedral layers (Table 3.1). Kaolinite, a 1:1 phyllosilicate, has very little tetrahedral or octahedral substitution (Thomas, 1998). Low charge afforded by low substitution is enhanced by hydrogen bonding between the tetrahedral and octahedral layers. This bonding holds 1:1 layers tightly together leaving little to no interlayer space for adsorption of cations or water (Dixon, 1989). Thus, Kaolinite is a non-expansive mineral.

Table 3.1: Chemical composition and layer charge of Common clay minerals (from Thomas, 1998).

Minerals	Chemical Formula	Charge per unit cell (equivalents moles ⁻¹)		Layer Charge
		Tetrahedral substitution	Octahedral substitution	
Kaolinite	$\text{Si}_4\text{Al}_4\text{O}_{10}(\text{OH})_8$	0	0	0
Muscovite	$\text{K}_2(\text{Si}_6\text{Al}_2)\text{Al}_4\text{O}_{20}(\text{OH})_4$	-2.0	0	-2.0
Vermiculite	$\text{Ca}_{1.48}(\text{Si}_{7.12}\text{Al}_{0.88})(\text{Al}_{2.8}\text{Mg}_{0.6}\text{Fe}_{0.6})\text{O}_{20}(\text{OH})_4$	-0.88	-0.66	-1.48
Montmorillonite	$\text{Ca}_{0.66}\text{Si}_8(\text{Al}_{3.34}\text{Mg}_{0.66})\text{O}_{22}(\text{OH})_4$	0	-0.66	-0.66

Mica is a 2:1 clay mineral with extensive solid state substitution of Al^{3+} for Si^{4+} in the tetrahedral layers. This substitution gives mica a layer charge of about 2. Non-hydrated K^+ binds adjacent tetrahedral layers because it is of the correct size and coordination to occupy the “holes” in the tetrahedral layer, electrostatically cementing the adjacent layers (Fanning et al., 1989). Although mica has a high layer charge, the tight bonding afforded by the K causes the mica to behave similarly to a kaolinite. The layers are bound together tightly allowing for little to no

interlayer space for adsorption of cations or water, thus mica is a non-expansive mineral (Thomas, 1998). Vermiculite does not have as much tetrahedral substitution of Al^{3+} for Si^{4+} as does mica and thus has a layer charge of 1 to 2 (Douglas, 1989). As a result, the interlayers of vermiculite are accessible to both cations and water. However, interlayer expansion is limited because vermiculite can adsorb only two layers of water. Conversely, montmorillonite is a highly expansive mineral. Most of the ionic substitution occurs in the octahedral layer, giving smectites a lower layer charge than vermiculite averaging about 0.5 to 1 (Thomas, 1998). The layers are bound together by very weak hydrogen bonds (easily broken) with little binding by interlayer cations giving montmorillonite the potential to adsorb many layers of water (Borchardt, 1989).

3.4 Methods used and results of this study

3.4.1 X-Ray diffraction (XRD)

3.4.1.1 Introduction

X-ray diffraction (XRD) is the primary method for identifying clay minerals as well as other minerals. Many authors used this technique in the identification of clay minerals (Moore and Reynolds, 1989; Harvey and Browne, 1991 and Jasmund and Lagaly, 1993).

In many geological investigations, XRD complements other mineralogical methods, such as microscopic studies, electron microprobe microscopy and scanning microscopy.

3.4.1.2 XRD Results

In this study, X-ray diffraction analyses are based on the collected representative samples from Gehannam Formation and Quaternary deposits for the determination of the clay and non clay mineral contents using three states, air dried, ethylene glycol and heating at 550°C. The

Instrument used (BRUKER D8 ADVANCE) was employed under the conditions of Target CU K α with secondary monochromator ($k\alpha = 40$, $Ma = 40$ mA). Minerals identified in the studied samples include, kaolinite, illite/smectite mixed layers, illite, calcite, quartz, gypsum, albite and minor amounts of halite present in few of the samples.

3.4.1.2.1 Non Clay Minerals

Non clay minerals contents in the studied Gehannam Formation and Quaternary deposits samples are mainly calcite, gypsum, quartz, albite and halite (Figs. 3.1 and 3.2).

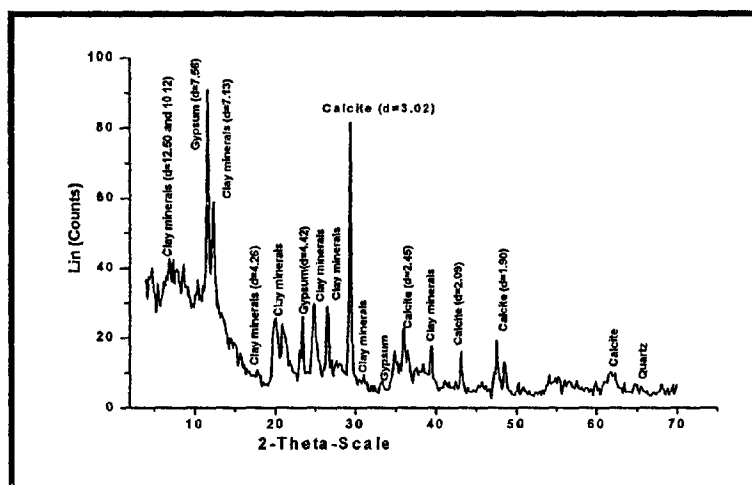


Fig. 3.1: X-Ray diffraction diagram in studied Gehannam Formation (Sample No. A₁).

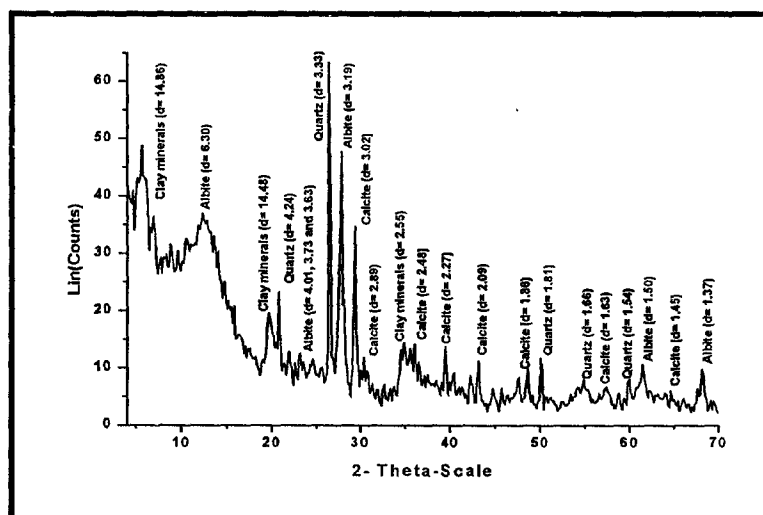


Fig 3.2: X-Ray diffraction diagram in studied Quaternary deposits (Sample No. B₅).

3.4.1.2.1. 1 Calcite

Calcite forms one of the most abundant non clay mineral in the samples derived from Gehannam Formation. It is identified by its distinctive reflections at 3.02 Å, 3.03 Å, 2.27 Å and 2.48 Å. On the other hand, calcite occurs in fewer amounts in the Quaternary samples (Figs. 3.1 and 3.2). Taces of dolomite also are observed in Gehannam Formation samples.

3.4.1.2.1. 2 Gypsum

Gehannam Formation samples have considerable amount of gypsum that is identified by its reflections at 4.42 Å and 3.9 Å (Fig. 3.1).

3.4.1.2.1. 3 Quartz

Quartz occurs in fewer amounts in both of Gehannam Formation samples and Quaternary deposits samples (Figs. 3.1 and 3.2) and it is characterized by distinctive reflections at 3.33 Å, 4.24 Å with some less strong peaks at 1.81 Å and 1.73 Å.

3.4.1.2.1. 4 Albite

Albite exists in very few samples of Gehannam Formation and it is identified by its reflections at 2.83 Å and 3.20 Å, but Quaternary deposits samples have considerable amount of Albite (Fig. 3.2).

3.4.1.2.1. 5 Halite

Trace amount of halite are observed in Gehannam Formation and it is identified by reflections at 2.82 Å and 1.99 Å.

3.4.1.2.2 Clay minerals

The clay samples in oriented mounts were run under three separate conditions, (Moore and Reynolds, 1989) (Figs. 3.3 and 3.4). I) Air dry state, II) After ethylene glycol treatment and III) After heating to 550°C for 1 hour. Clay minerals contents in the studied Gehannam Formation

and Quaternary deposits samples are Kaolinite, illite and illite/smectite mixed layer (Table. 3.2)

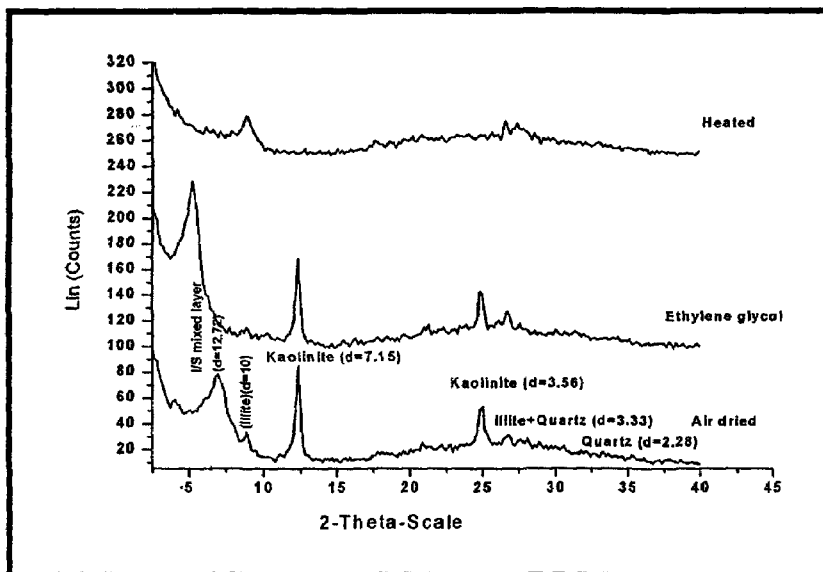


Fig. 3.3: X-Ray diffraction diagram at the air-dried, ethylene glycol and heating states in studied Gehannam Formation (Sample No. B₁₋₁).

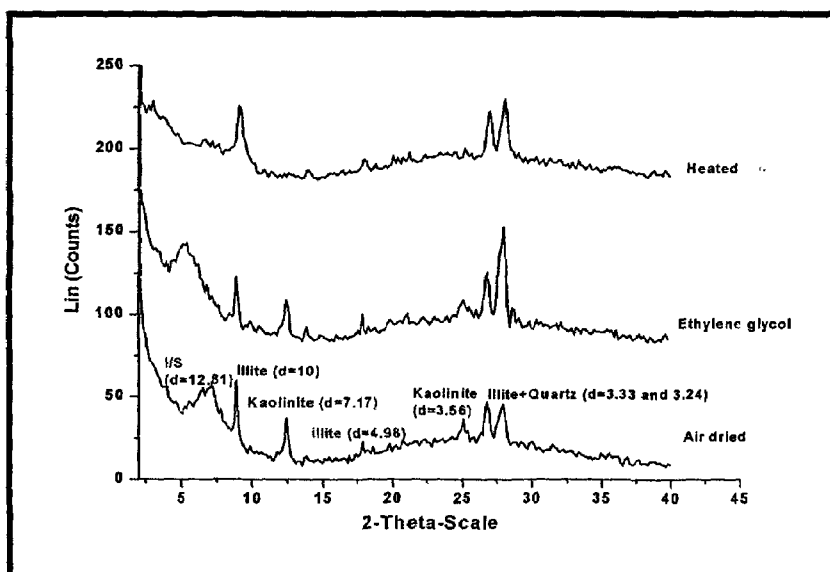


Fig. 3.4: X-Ray diffraction diagram at the air-dried, ethylene glycol and heating states in Quaternary deposits (Sample No. B₅).

Table 3.2: Shows clay minerals percentages in both Gehannam Formation samples and Quaternary deposits samples.

Minerals content	Kaolinite (%)	Illite (%)	I/S (%)	Smeectite (%) in mixed layer	Total illite (%)
Gehannam Formation	55	12	34	24	23
Quaternary deposits	25	55	23	17	61

3.4.1.2.2. 1 Kaolinite

Kaolinite is the most abundant clay mineral in Gehannam Formation samples (Table. 3.2) and it is represented by a basal (001) reflections at 7.13 Å, 7.17 Å and 3.56 Å in air dried state which show no change with glycolation but the collapse of the kaolinite structures to an amorphous material take place on heating to 550°C indicated by the disappearance of kaolinite peaks (Figs. 3.3 and 3.4).

3.4.1.2.2. 2 Illite

Illite is identified by series of reflections at 10 Å, 3.33 Å and 3.24 Å. Its peaks are stable at the three mentioned states. With the heating to 550°C, the 001 peak of illite shows no change or a slight collapse (Figs. 3.3 and 3.4). Values of less than 10 Å may be due to a K⁺ deficiency or the substitution of Fe²⁺ or Mg²⁺ for [Al³⁺] (Güven et al., 1980).

3.4.1.2.2. 3 Interstratified Illite/Smeectite mixed layer

Illite smectite mixed layer (I/S) clay is identified by its reflections at 12.7 Å and 12.8 Å at air dried state, it expands to higher spacing upon glycolation and collapse to 10 Å on heating to 550°C (Figs. 3.3 and 3.4).

The expandability and thereby the percentage of smectite in mixed layer clay minerals was calculated according to Weaver (1956) as shown in Fig. 3.5 by determining the peak intensity of the mixed layer in ethylene glycol state. From Figs. 3.3 and 3.4, it is found that 2θ of the peaks in both Gehannam Formation and Quaternary deposits samples in glycolated state are 5.5 degree for Illite/Smeectite mixed layer which

corresponding to the peak intensity of 16.5 Å. By plotting the value 16.5 Å of expandable layer on Weaver (1956) diagram (Fig. 3.5), it intersects the curve at 70% on the expandable portion axis and the percentages of smectite in mixed layer are calculated (Table 3.2).

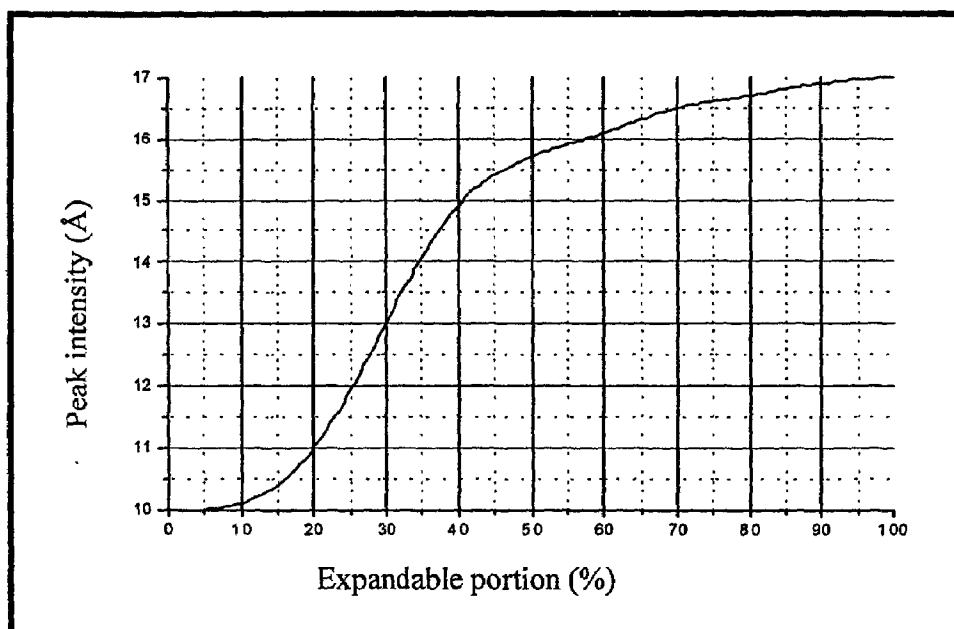


Fig. 3.5: Determination of expandable portion of mixed layer clay minerals after treatment with ethylene glycol

The percentages of smectite, illite within mixed layer and total illite for Gehannam Formation and Quaternary deposits can be calculated as follows:

Smectite % = {(Expandability estimated from Fig. 3.5) X I/S %} /100.

Consequently Illite % within mixed layer = I/S mixed layer % - Smectite % within mixed layer. Total illite can be calculated as the sum of illite % within I/S mixed layer and individual illite % (Table 3.2).

According to the clay mineral contents, the rock materials and their weathering products can be classified into two groups:

1-Illite, kaolinite and illite/smectite mixed layers bearing Quaternary deposits.

2-Kaolinite and illite/smectite mixed layers with illite bearing Gehannam Formation.

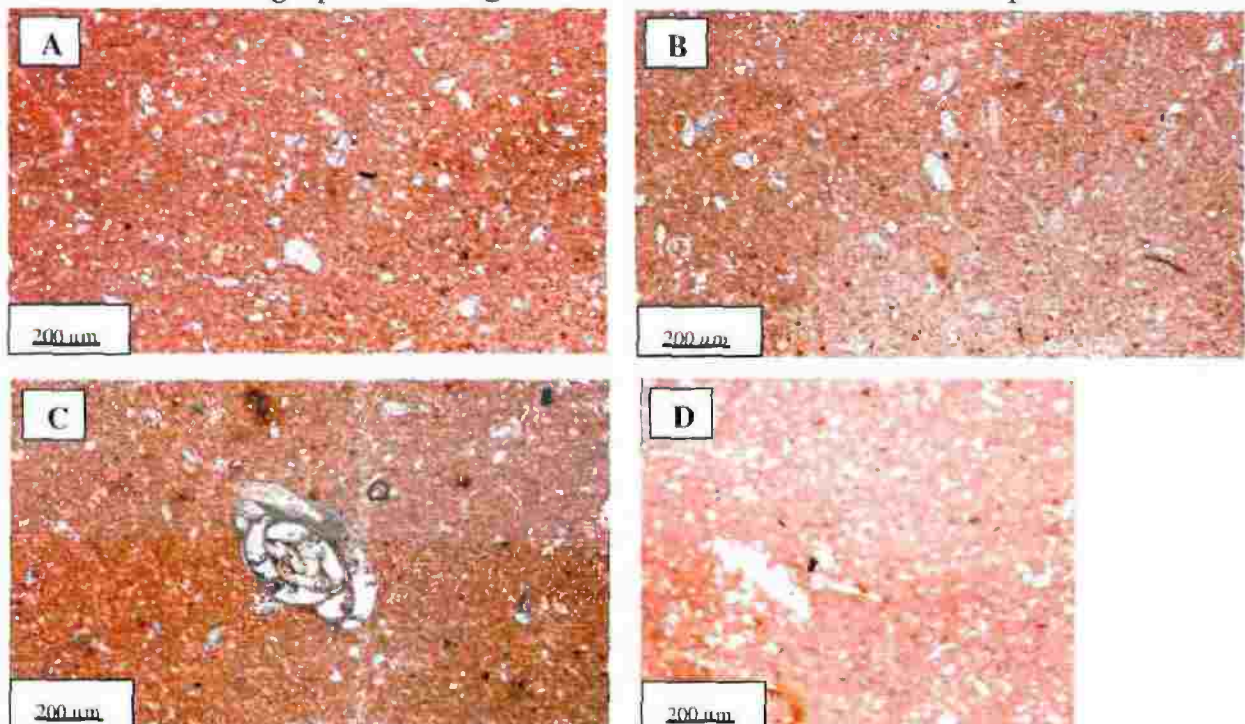
3.4.2 Petrography

Thin section microscopy is one method used to study the textural features and to identify some minerals of mudrocks (Mackenzie and Guilford, 1980; Shelley, 1985 and Nesse, 1991). The distinction between various types of clay minerals by this technique is difficult because of their similarity in optical properties. The mineralogical constituents of Gehannam Formation samples and Quaternary deposits in the present study as shown in plates 1 and 2 are described as follows:

1-Gehannam Formation is represented by argillaceous fossiliferous biomicrite (Wackestone) showing:

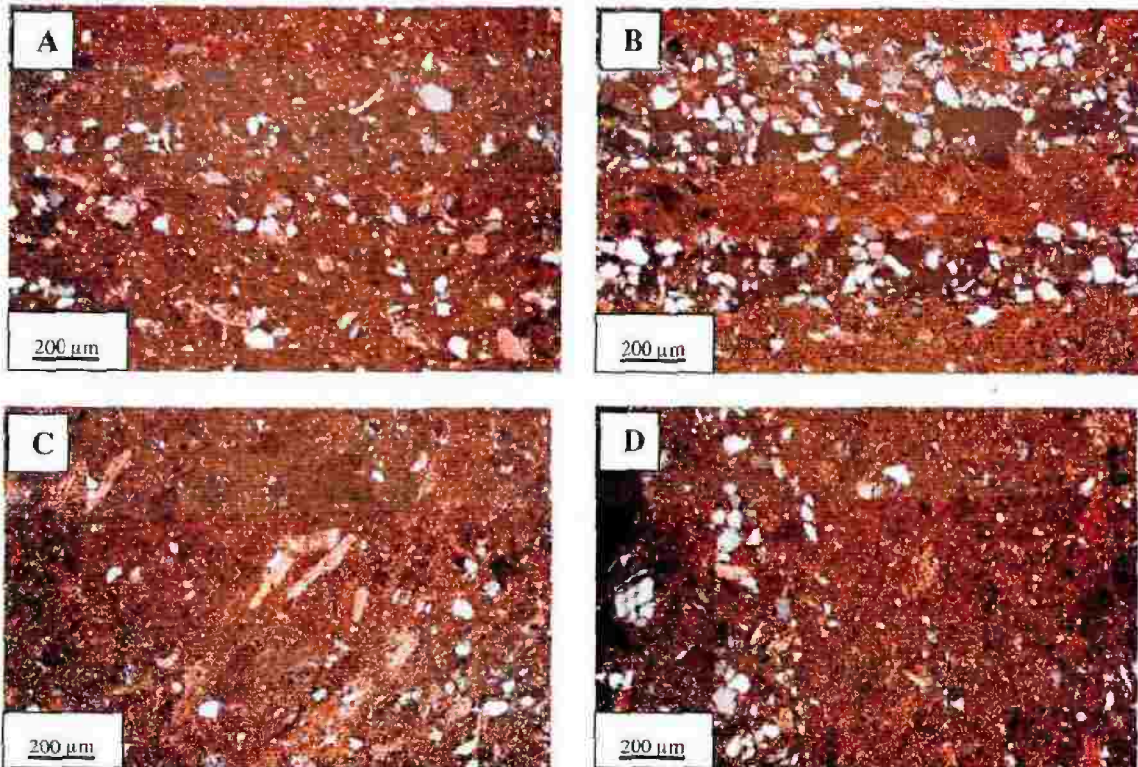
- A- Small size shell fragments embedded in a micrite groundmass.
- B- Preferred orientation of microsparite within a micrite groundmass.
- C- Sparite crystals within shell fragments in a micrite groundmass.
- D- Two generations of carbonates, sparite (fossils) and micrite groundmass.

Plate 1: Petrographic investigation of Gehannam Formation samples.



2-Quaternary deposits (Plate 2), A, B and C are sandy calcareous mudstone showing, laths of mica (C) and microcline grains in the sand size (D). Sandy calcareous shale (B), showing lamination of light bands (fine sand) and dark bands (clays)

Plate 2: Petrographic investigation of Quaternary deposits samples.



3.4.3 Scanning electron microscope (SEM)

3.4.3.1 Introduction

By scanning with an electron probe across a specimen, high resolution images of the morphology or topography of a specimen at various magnifications can be obtained. The scanning electron microscope (SEM) equipped with an energy dispersive X-ray analysis system (EDX). Compositional analysis of the samples under consideration can be obtained by monitoring secondary X-rays produced by the electron-specimen interactions (EDX). Thereby details of the distribution and concentration of elements can be obtained. By comparison the relative concentrations of the elements with the crystal morphology, the chemical formula of a suspected mineral may be derived (Welton, 1984; Deer, et al., 1966; 1978 and 1997).

A Scanning electron microscope (SEM) has been used in the present study. The very high resolution obtained in the SEM readily describes the minerals. The analyses also reveal their morphology and textural relationship. SEM analyses were carried out with magnifications between 270X and 3300X with Au-Pb coated samples. The description of the micrographs is based on SEM micrographs and EDX analysis. Identification of structural features and mineral chemistry has been studied by comparison of the micrographs and EDX spectra with those shown in the Welton atlas (1984).

3.4.3.2 Gehannam Formation

The clay minerals constituents within Gehannam Formation include minerals such as illite, illite/smectite mixed layers and kaolinite (Figs. 3.6, 3.8, 3.9, 3.10 and 3.11). Non clay minerals contain K-feldspar, carbonate minerals and quartz crystals (Figs. 3.6, 3.7, 3.12, 3.13 and 3.14).

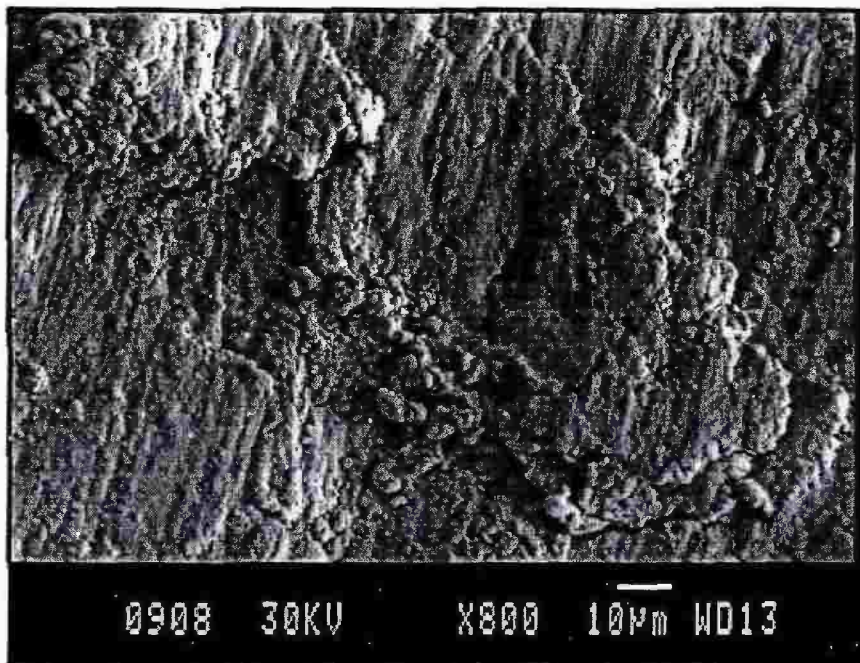


Fig. 3.6: SEM micrograph of fringe like shape of illitic ribbons which appear as shiny lines and preferred orientation of K-feldspar, Gehannam Formation (Sample No. C_{2.4}).

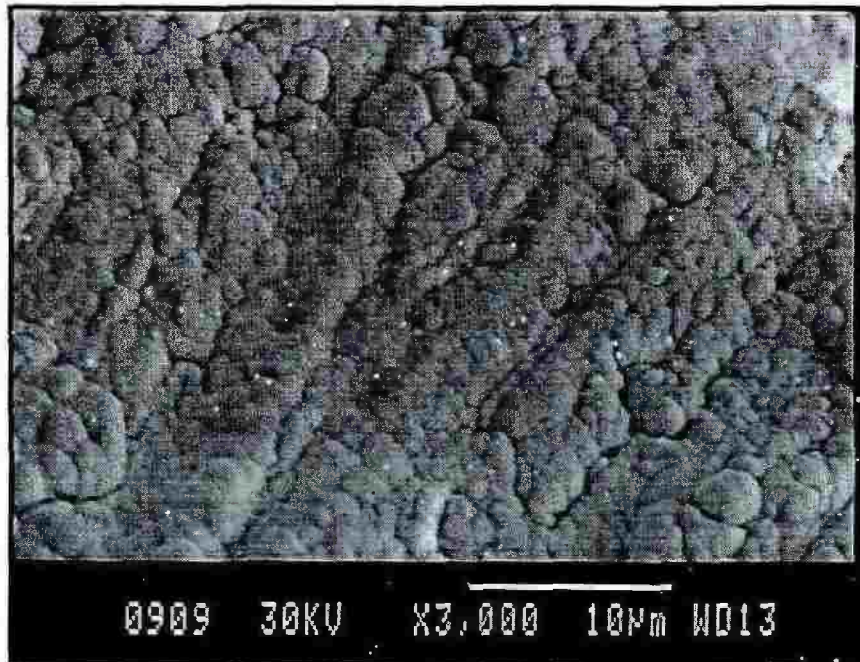


Fig. 3.7: Enlargement of Fig (3.6) revealed K-feldspar and its alteration product marked by preferred orientation.

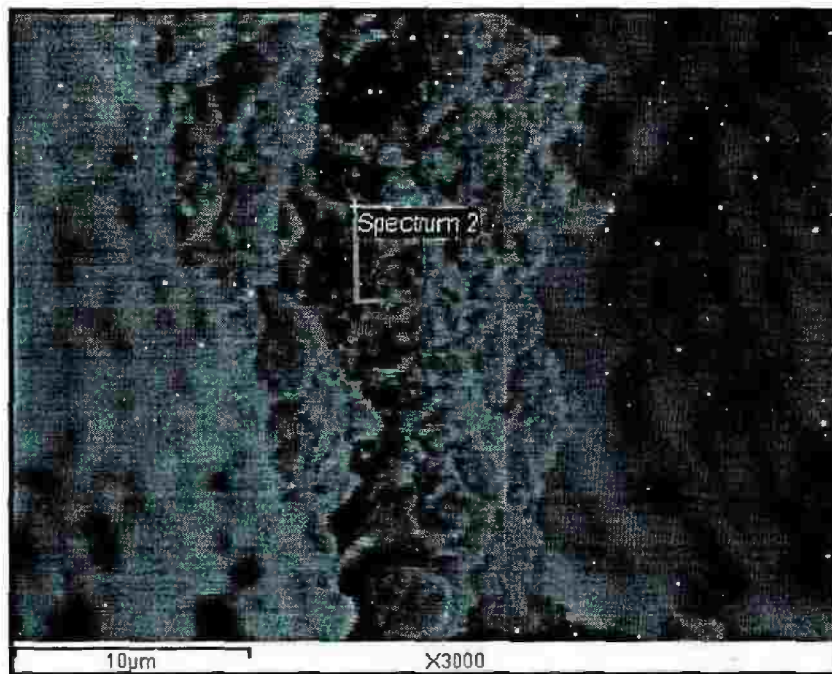


Fig. 3.8: SEM micrograph show thin ribbons of filamentous illite/smectite mixed layers in Gehannam Formation (Sample No. C2-4), similar examples of this type are shown in Welton Atlas (1984).

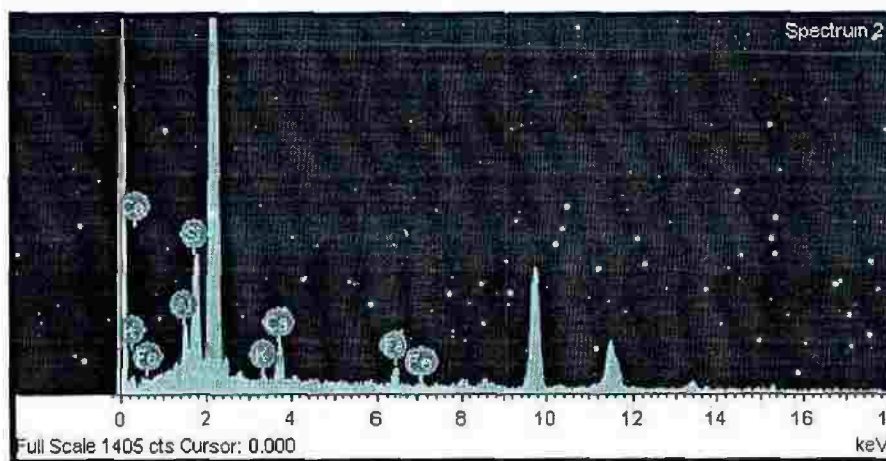


Fig. 3.9: Energy dispersive X-ray (spectrum 2) from an area indicated on Fig (3.8) showing the major elements are Si, Al, Ca, K, and Fe.

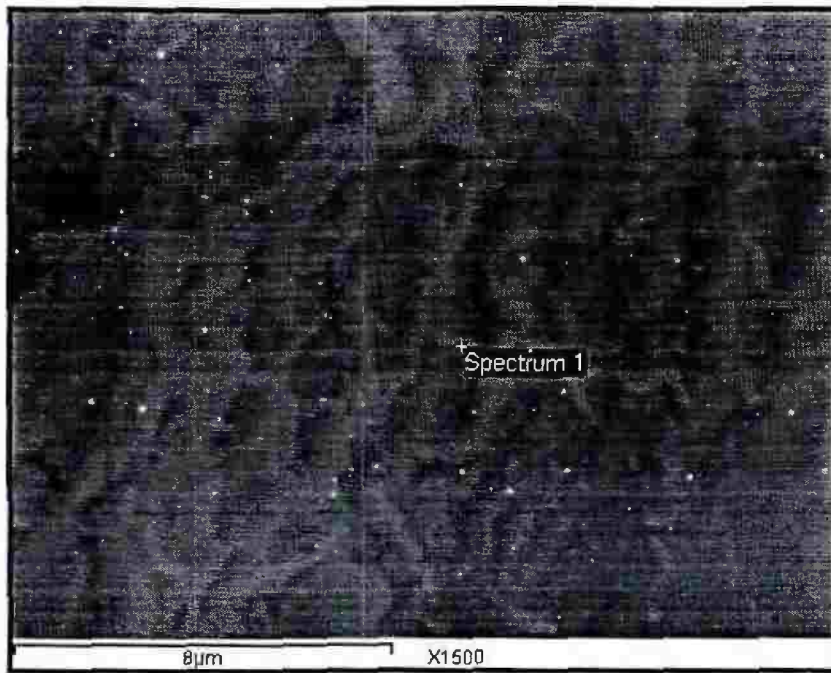


Fig. 3.10: SEM micrograph of illite/Smectite mixed layer in Gehannam Formation emphasized by EDX results in Fig. 3.9 (spectrum 1).

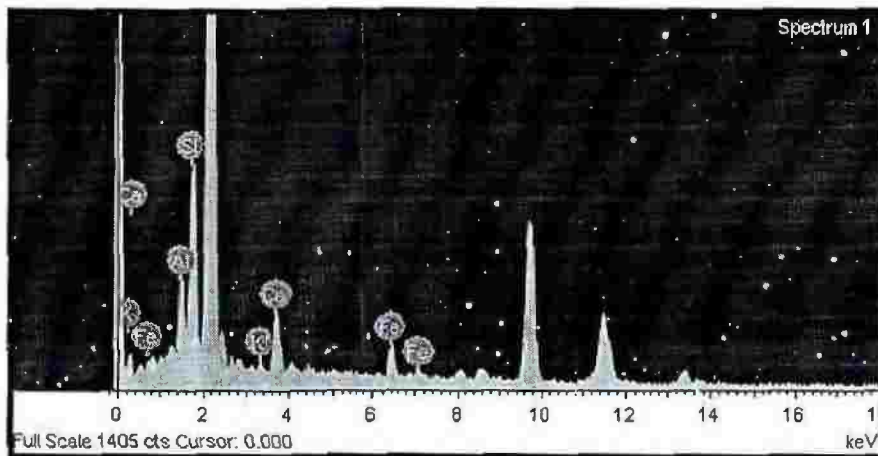


Fig. 3.11: Energy dispersive X-ray spectrum (1) from an area indicated on Fig. 3.10 showing the major elements of illite/smectite mixed layer.

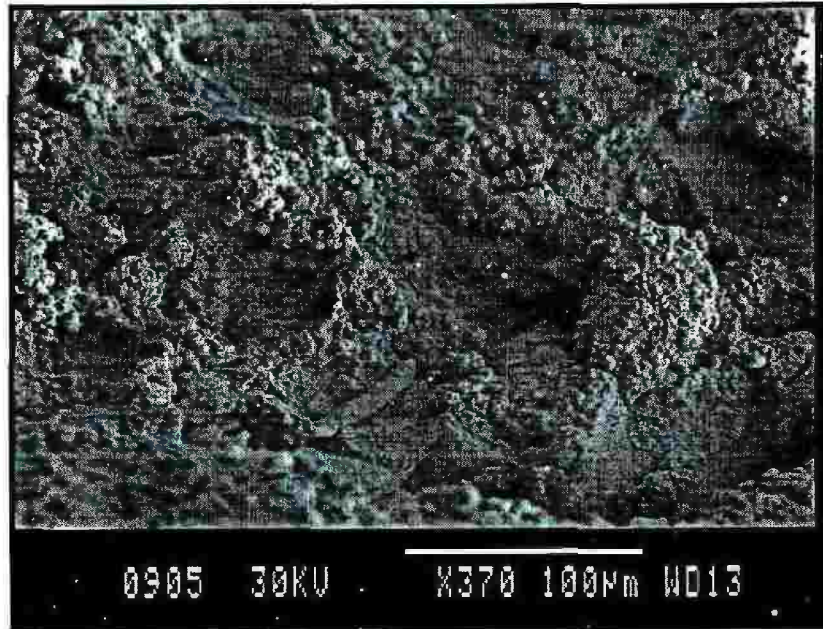


Fig. 3.12: SEM micrograph of carbonate, small rounded quartz. Gehannam Formation (Sample No. C₂₋₂).



Fig. 3.13: Enlargement of Fig. 3.12, the selected area on the image shows rhombohedral calcite crystals.

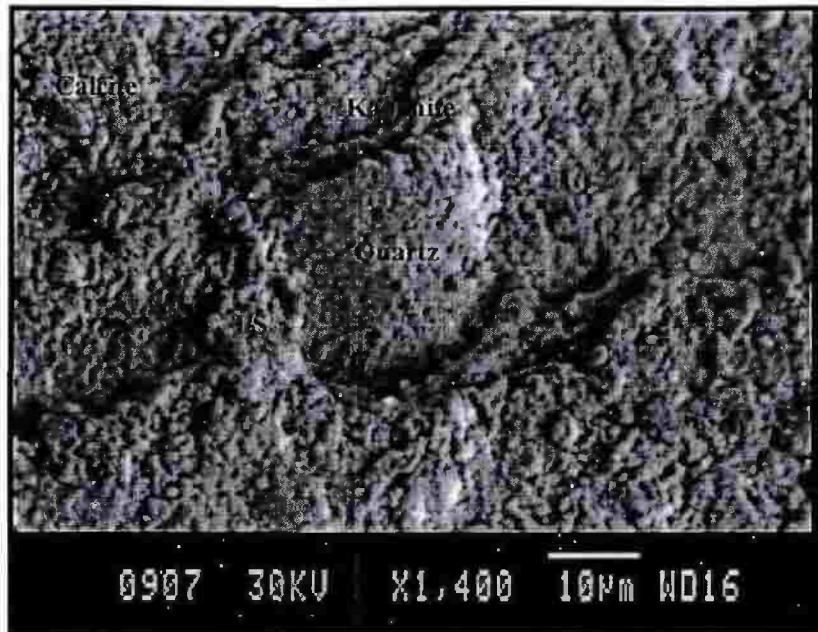


Fig. 3.14: SEM micrograph show rhombohedral calcite, quartz grain, kaolinite and illite/smectite in prephery of quartz grains (Sample No. C₂₋₃).

Illite clay minerals in Gehannam Formation samples found as fringe ribbons shape as the intensive weathering of euhedral cleavable crystals of K-feldspar crystals (Figs. 3.6 and 3.7). Illite/smectite mixed layer clay minerals occur as ribbons filamentous needle crystals like shape according to the description given by welton, 1984 with high distribution of major elements like Si, Al, Ca and Fe (Figs. 3.8, 3.9, 3.10, 3.11 and 3.14). Carbonate minerals occur as rhombhedral crystal of calcite and dolomite (Fig. 3.13). Finally quartz occurs as rounded to oval shape crystals (Figs. 3.12 and 3.14).

3.4.3.3 Quaternary deposits

The Quaternary deposits composed mainly of clay minerals mainly kaolinite, illite as well as K-feldspar (Figs. 3.15, 3.16, 3.17, 3.18, 3.19, 3.20, 3.21 and 3.22). Kaolinite clay mineral occurs mainly as pseudo-hexagonal plates or book-like shape (Figs. 3.15 and 3.17). The weathering of K-feldspar and its replacement by kaolinite are illustrated in Figs. 3.15 and 3.17. Blocky crystal of

K-feldspar embedded in the clay minerals groundmass is also observed with its weathering products to kaolinite clay minerals (Figs. 3.15 and 3.17). Illite clay minerals are also the major constituents in Quaternary deposits samples and occur as flaky and sheet like crystals (Figs. 3.15, 3.17, 3.19 and 3.21). Si, Al, K, Ca, Fe and Ti are the chemical constituents of the illite crystals (Figs. 3.20 and 3.22). The occurrence of K in the illite minerals suggested that, it formed as the alteration of K-feldspar due to the relative peak height of K is more or less approached the peak height of Al (Fig. 3.22).

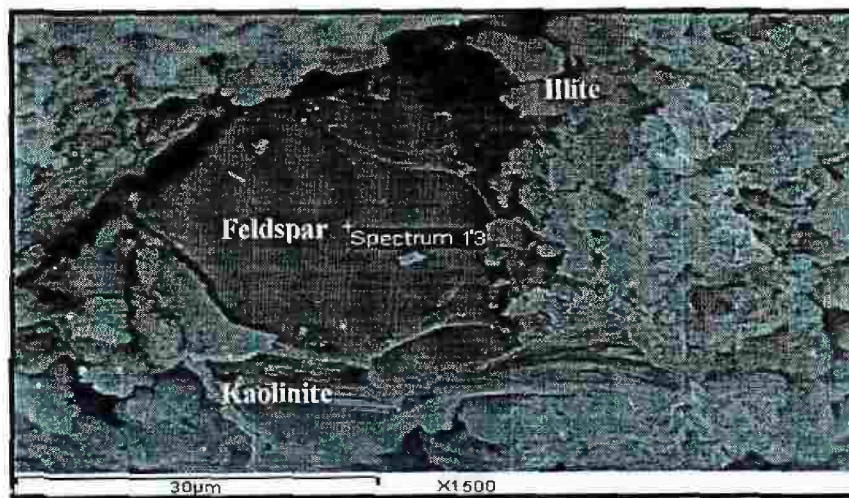


Fig. 3.15: Blocky shaped feldspar embedded in groundmass of flaky-like shape illite, feldspar show some alteration at its lower rims to kaolinite with book-like shape (Quaternary deposits).

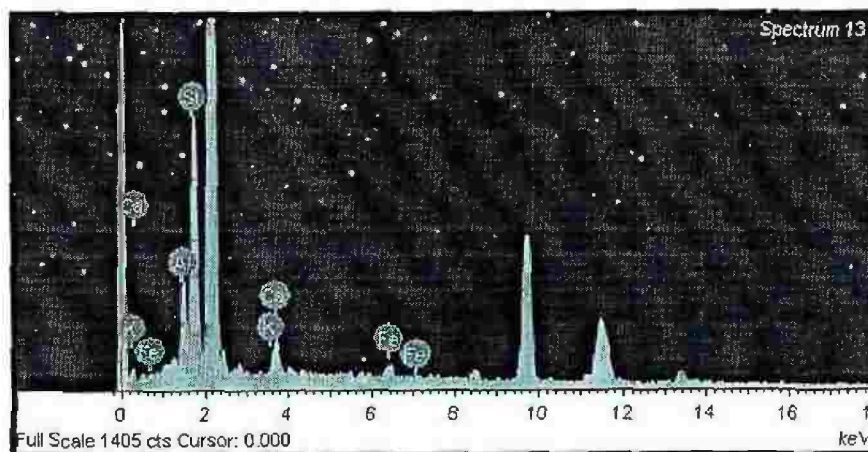


Fig. 3.16: Energy dispersive X-ray spectrum from an area indicated on Fig. 3.15 indicative of K-feldspar where the relative peak heights of the major elements match with the chemical formula of the K-feldspar (K: Al: Si: 1:1:3).

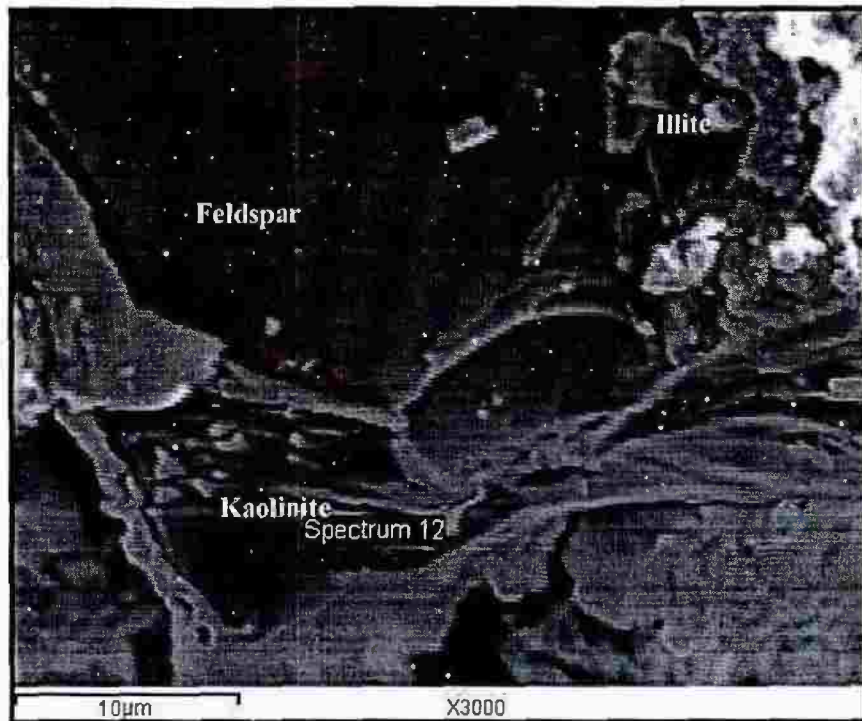


Fig. 3.17: Blocky shaped feldspar embedded in groundmass of flaky- like shape illite, feldspar crystal shows some alteration at its lower rims to kaolinite identified by its book- like shape (Quaternary deposits).

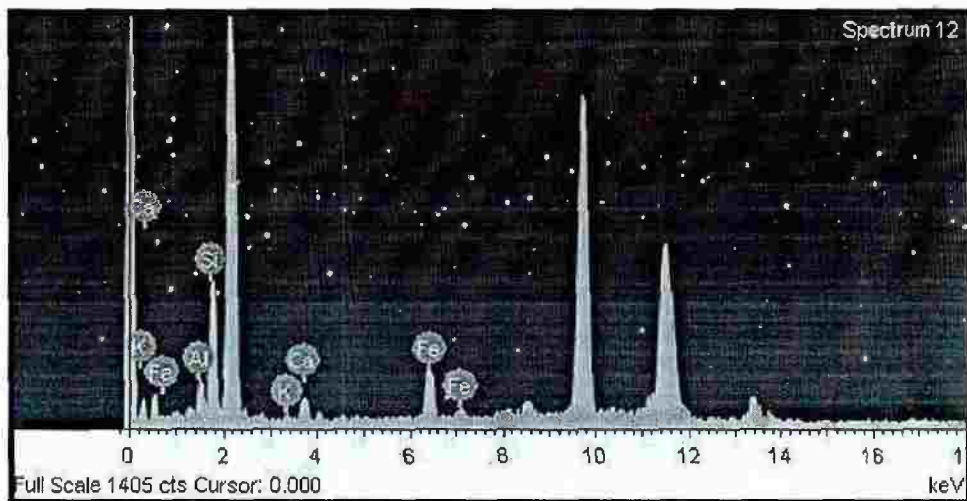


Fig. 3.18: Energy dispersive X-ray spectrum from an area indicated on Fig. 3.17 the EDX spectrum contains all the major elements (Si, Al and K) typical of K-feldspars.

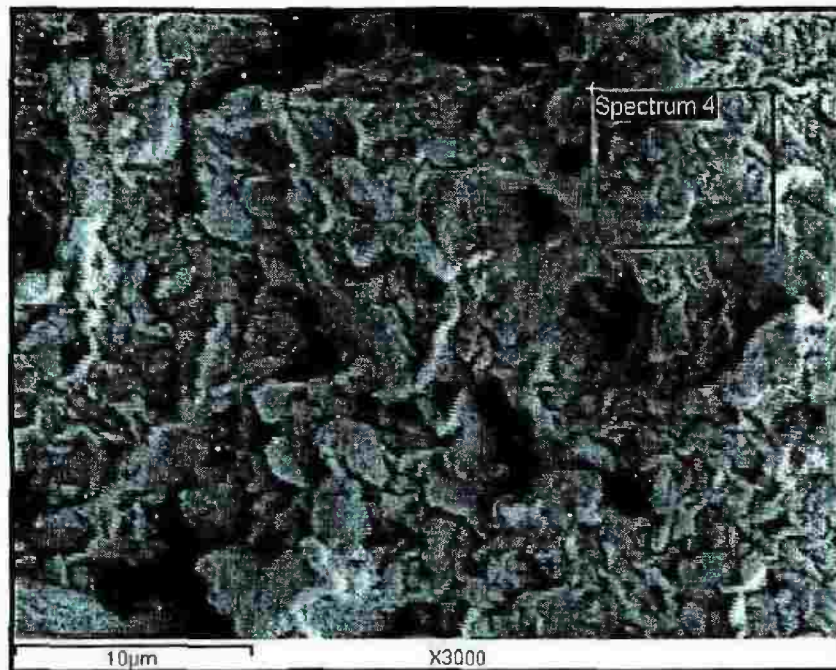


Fig. 3.19: Massive detrital illite composed of irregular, flake like caly. The Welton atlas (1984) shows similar example of this type.

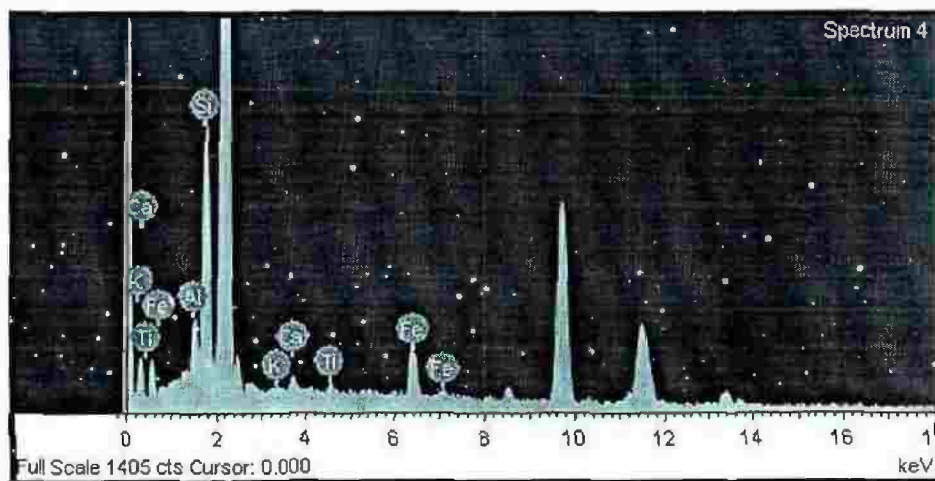


Fig. 3.20: Energy dispersive X-ray spectrum from an area indicated on Fig (3.19), the EDX matches with the chemical formula of illite except for the presence of minor amount of Ti and Ca. and presence of Fe may be due to iron oxide coating as result of oxidation as chemical weathering (Quaternary deposits).

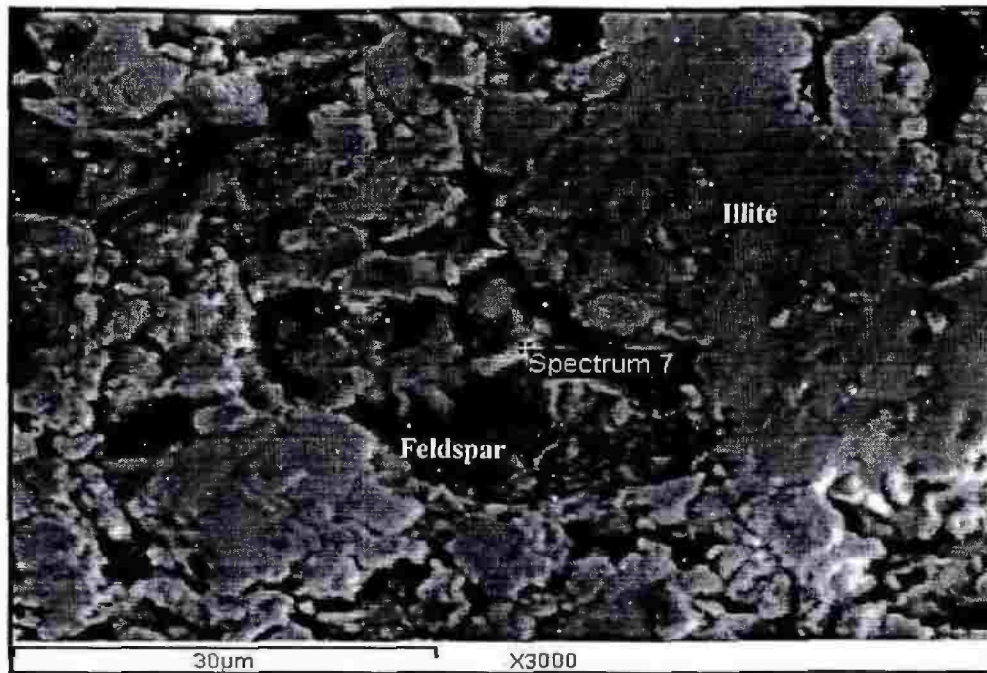


Fig. 3.21: SEM micrograph shows feldspar immersed within sheet-like shape of illite (Quaternary deposits).

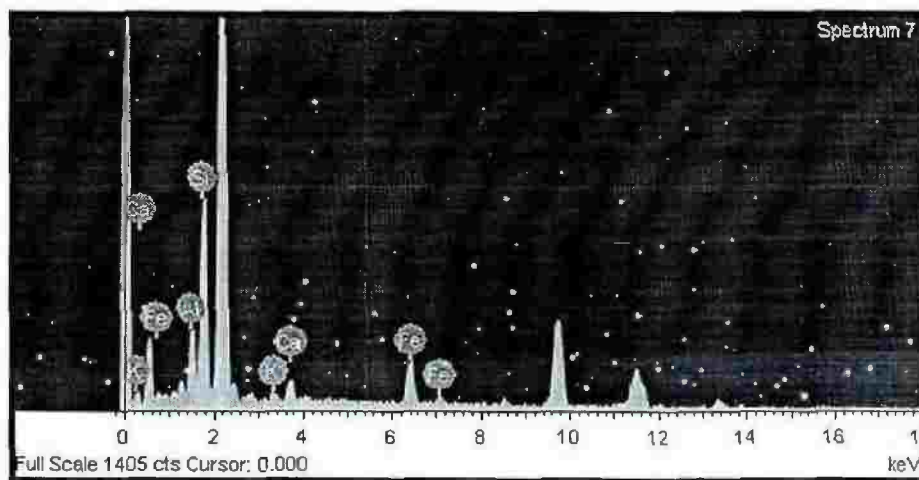


Fig. 3.22: Energy dispersive X-ray spectrum from an area indicated on Fig. 3.21 matches with the formula of illite, where the relative peak height of K is usually less than that of Al, this is in contrast to K-feldspar where the K and Al peaks are of equal height.

3.4.4 Geochemistry

3.4.4.1 Introduction

The present work is based on chemical analysis data of major and trace elements in the samples collected from the Gehannam Formation and Quaternary deposits. The analysis was done by X-ray fluorescence (XRF) using wavelength dispersive spectrometer (Axios Advanced, PANalytical 2005). Data were processed by the software (IQ+ and Super Q). The obtained results are quoted in tables 3.3 and 3.4.

The contents of the carbonate fraction and the insoluble residue have been calculated empirically (Table. 3.3). According to relative quotients of the carbonate, insoluble residue and iron oxides, the studied sediments can be classified into:

- 1- Ferriferous argillaceous limestone (B₁₋₁)
- 2- Limestone (C₁)
- 3- Calcareous shale (C₂₋₃)
- 4- Ferriferous Calcareous shale (C₂₋₄, C₄ and B₅).

3.4.4.2 Major oxides in relation to clay mineralogy:

The Si/Al ratio ranges between 1:2 to 1:3 which corresponds to clay minerals having three-layer structure (TOT) (Table. 3.3 and Fig. 3.23). The positive relation between Al₂O₃ and K₂O (Fig. 3.24) can be held as an indication of dominant illite variety in both Gehannam Formation and Quaternary deposits. These observations agree fairly well with the data published by Liu, et al., 2000. The K₂O/Al₂O₃ ratio is higher in the Quaternary deposits than those of Gehannam Formation, suggesting more illitic character for the former. The SiO₂/Al₂O₃ ratio exceeds the limit 3 for the Quaternary deposits suggesting possible free-silica (quartz) admixture. Petrographically, the Quaternary sediments are relatively enriched in detrital quartz.

Table 3.3: Major oxides abundances in the investigated Gehannam Formation and Quaternary deposits, B₁₋₁, C₁, C₂₋₃ and C₂₋₄ are Gehannam samples while C₄ and B₅ are Quaternary samples.

Formation	Sample No.	SiO ₂	TiO ₂	Al ₂ O ₃	Fe ₂ O ₃	MnO	MgO	CaO	K ₂ O	Na ₂ O	P ₂ O ₅	SO ₃	LOI	Si/Al	Carbonate (%)	Insoluble residue
Gehannam	B ₁₋₁	25.24	0.55	10.55	6.55	0.06	0.64	26.10	0.61	0.92	0.39	0.43	27.87	2.4	46.61	36.40
	C ₁	7.63	0.21	2.65	2.45	0.06	0.53	41.95	0.29	1.61	0.23	0.58	41.46	2.9	74.91	10.57
	C ₂₋₃	41.24	0.79	18.12	0.08	0.07	0.94	11.47	0.80	0.45	0.17	0.10	18.6	2.3	20.48	60.16
	C ₂₋₄	36.11	0.93	16.60	10.55	0.01	0.69	13.24	0.84	0.50	0.16	1.43	18.89	2.18	23.64	53.55
Quaternary	C ₄	50.91	1.44	15.25	12.13	0.09	0.85	4.04	0.84	0.45	0.31	0.17	13.53	3.3	7.21	67.00
	B ₅	50.77	1.46	13.41	9.52	0.18	1.33	7.70	1.00	0.69	0.21	0.12	13.16	3.79	13.75	65.18

Table 3.4: Average of the trace elements distribution in the investigated Gehannam Formation and Quaternary deposits.

Elements ppm.	Ba	Cr	Co	Ni	Nb
Gehannam	362.0	153.00	74.3	86.30	18.0
Quaternary	370.5	125.50	37.0	73.50	18.0

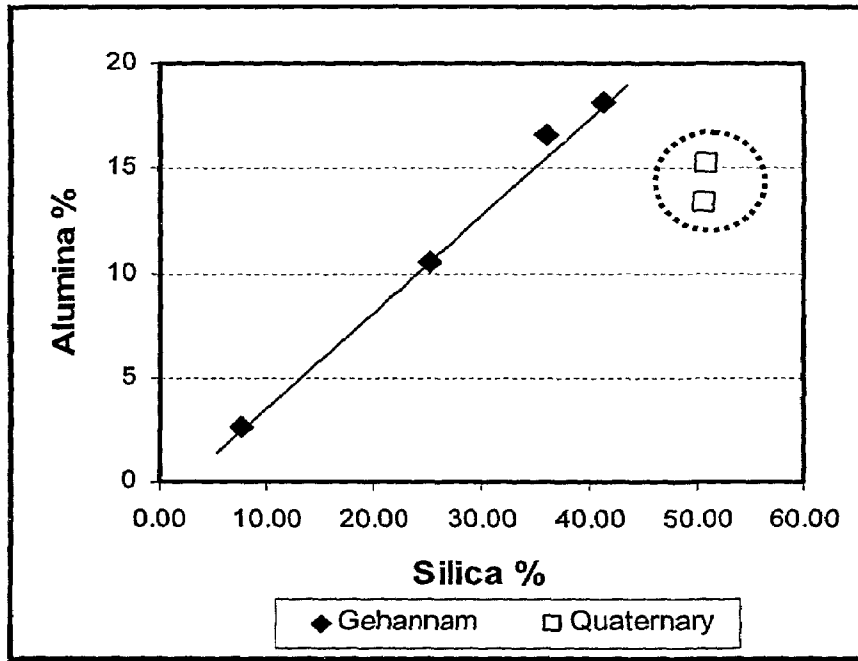


Fig. 3.23: Positive relationship between SiO_2 and Al_2O_3 in the analyzed sediments of the Gehannam Formation and Quaternary deposits.

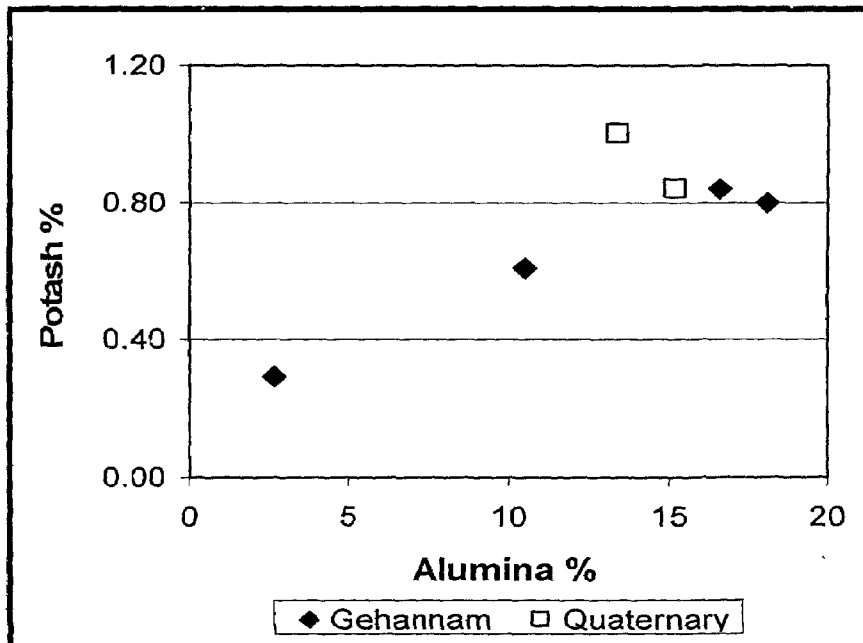


Fig. 3.24: Positive relationship between Al_2O_3 and K_2O in the analyzed sediments of the Gehannam Formation and Quaternary deposits.

3.4.4.3- Weathering products:

The study is based on samples collected from surface exposures; hence avoiding the effect of chemical weathering is not possible. The collected limestones and marls of the Gehannam Formation are intersected by numerous streaks, band and veinlets filled by gypsiferous material. The secondary filling by such gypsiferous material (syntexial) is always associated with marked impregnation by ferruginous materials (iron oxy-hydroxides). The straightforward explanation of such features can be interpreted to weathering of sulfides precursor, such as pyrite.

The relative preponderance of these weathering products, namely; gypsiferous and ferruginous materials, suggests that pyrite (and possibly other sulfides) is abundant in the non-weathered sediments. The presence of sulfides is an indicator of anoxic depositional environments which favor, in turn, the preservation of organic matter. Accordingly, the writer would suspect that the Gehannam sediments are possible source rock enriched in both organic matter and sulfides.